ISI Web of SCIENCE® Powered by ISI Web of Knowledge℠
HOME HELP DATE & DB LIMITS GENERAL SEARCH CITED REF SEARCH COMBINE SEARCHES ADVANCED SEARCH

General Search Results--Full Record

Article 1 of 1

☐ MARK

Airborne **measurements of aerosols from burning biomass in Brazil related to the TRACE a experiment**

Pereira EB, **Setzer AW**, Gerab F, Artaxo PE, Pereira MC, Monroe G

JOURNAL OF GEOPHYSICAL RESEARCH-ATMOSPHERES
101 (D19): 23983-23992 OCT 30 1996

Document type: Article **Language:** English **Cited References:** 25 **Times Cited:** 18 FIND RELATED RECORDS Explanation

Abstract:
Results are reported from an **airborne** campaign to investigate the impacts of burning biomass upon the loading of lower-tropospheric aerosols and its composition over the Brazilian tropics. The flights, conducted as part of the NASA/Transport and Atmospheric Chemistry Near the Equator-Atlantic (TRACE A) mission, started on September 1, 1992, when the dry (fire) season still prevailed in the central part of Brazil, and ended on September 29. Of the total number of burnings detected in Brazil by the advanced very high resolution radiometer (AVHRR)/NOAA satellite sensor, 74% were concentrated in the states of Amazonas, Maranhao, Mate Grosso, Para, Roraima, and Tocantins during this period. Aerosol particles were sampled from a twin-engine aircraft in transit and vertical profile flights were made up to 4,000 m altitude. Black carbon measurements made in real time and in areas of burning biomass peaked at similar to 2,500 m above the ground, increasing to similar to 12,000 ng/m(3). In other areas these values were lower by 1 order of magnitude. A condensation nuclei counter measuring small particles (>0.014 mu m) produced values ranging from 2,000 to 16,000/cm(3) for areas with low and high burning biomass, respectively. Deposition filters in a two-stage cascade impactor, and Nuclepore filters collected aerosols for analysis of 13 elements through particle-induced X ray emissions (PIXE). Primary elements associated with soil dust (Al, Si, Mn, Fe, Ni) prevailed in the aerosol coarse mode (>1 mu m) while the fine mode aerosols were enriched in S, K, Br, and Rb, which are tracers normally associated with burning of biomass. The good correlation between fire spot counts, obtained via AVHRR aboard NOAA satellites, and black carbon, counts of small particles and total aerosol mass, suggests the determining of local concentrations of fire-derived aerosol fire emissions by satellite to be a new and useful approach.

KeyWords Plus:
AMAZON BASIN, EMISSIONS, CARBON, SMOKE, TRANSPORT, SITES, FIRES

Addresses:
Pereira EB, INST NACL PESQUISAS ESPACIAIS,CP 515,BR-12201970 S JOSE CAMPOS,SP,BRAZIL
UNIV SAO PAULO,INST FIS,BR-05389 SAO PAULO,BRAZIL
FDN CEARENSE METEOROL & RECURSOS HIDRICOS,FUNCEME,BR-60325 FORTALEZA,CEARA,BRAZIL

Publisher:
AMER GEOPHYSICAL UNION, 2000 FLORIDA AVE NW, WASHINGTON, DC 20009

IDS Number:
VQ493

ISSN:
0148-0227

Article 1 of 1

Acceptable Use Policy

Copyright © 2004 Thomson ISI

JOURNAL OF GEOPHYSICAL RESEARCH, VOL. 101, NO. D19, PAGES 23,983–23,992, OCTOBER 30, 1996

Airborne measurements of aerosols from burning biomass in Brazil related to the TRACE A experiment

E. B. Pereira,[1] A. W. Setzer,[1] F. Gerab,[2] P. E. Artaxo,[2]
M. C. Pereira,[1] and G. Monroe[3]

Abstract. Results are reported from an airborne campaign to investigate the impacts of burning biomass upon the loading of lower-tropospheric aerosols and its composition over the Brazilian tropics. The flights, conducted as part of the NASA/Transport and Atmospheric Chemistry Near the Equator–Atlantic (TRACE A) mission, started on September 1, 1992, when the dry (fire) season still prevailed in the central part of Brazil, and ended on September 29. Of the total number of burnings detected in Brazil by the advanced very high resolution radiometer (AVHRR)/NOAA satellite sensor, 74% were concentrated in the states of Amazonas, Maranhão, Mato Grosso, Pará, Roraima, and Tocantins during this period. Aerosol particles were sampled from a twin-engine aircraft in transit and vertical profile flights were made up to 4,000 m altitude. Black carbon measurements made in real time and in areas of burning biomass peaked at ~2,500 m above the ground, increasing to ~12,000 ng/m^3. In other areas these values were lower by 1 order of magnitude. A condensation nuclei counter measuring small particles (>0.014 μm) produced values ranging from 2,000 to 16,000/cm^3 for areas with low and high burning biomass, respectively. Deposition filters in a two-stage cascade impactor, and Nuclepore filters collected aerosols for analysis of 13 elements through particle-induced X ray emissions (PIXE). Primary elements associated with soil dust (Al, Si, Mn, Fe, Ni) prevailed in the aerosol coarse mode (>1 μm) while the fine mode aerosols were enriched in S, K, Br, and Rb, which are tracers normally associated with burning of biomass. The good correlation between fire spot counts, obtained via AVHRR aboard NOAA satellites, and black carbon, counts of small particles and total aerosol mass, suggests the determining of local concentrations of fire-derived aerosol fire emissions by satellite to be a new and useful approach.

Introduction

Some 2 – 10 × 10^{15} g of dry biomass burn every year, 80% of which occurs in the tropics, producing large amounts of atmospheric pollutants [*Crutzen and Andreae*, 1990]. The resulting total emission of particulate matter from this source has been estimated at 10^{14} g/yr, with about half of the particulates in the fine mode (<2.0 μm in diameter); for elemental carbon the emission from burning biomass (2 × 10^{13} g) could account for up to ~86% of the total anthropogenic release [*Levine*, 1990].

About 97% of the aboveground carbon in a tropical forest is injected into the atmosphere from many fires over a 10-year period [*Fearnside et al.*, 1991] and more than ~85% of this carbon is released as CO_2 [*Ward*, 1990]. *Ward and Hardy* [1991] have described aerosol particles generated in different combustion phases, and *Ward et al.* [1992] and *Kaufman et al.* [1992] have made specific emission measurements in tropical forests, secondary forests, and savannas of Brazil in recent years. The overall emission factors they reported included the Brazilian data and varied from 5 to 40 g of particulates per kilogram of dry matter for corresponding combustion efficiencies, varying from 98 to 60%, respectively; high releases of other elements, among them Na, K, Cl, Ca, and S were also reported.

Artaxo and collaborators [e.g., *Artaxo et al.*, 1988, 1990, 1993a, b, 1994] focused on the elemental and size distribution analysis of natural and fire-related aerosols collected from ground monitoring stations and in controlled fires in forests and savannas of central Brazil and Amazon. They reported high levels of K, S, Si, Zn, and organic matter, as well as total environmental aerosol loads of ~600 μg/m^3, directly caused by burning biomass. For a savanna fire in southern Brazil, *Coutinho* [1990] summarized the percentage transfer of elemental mass from the above ground phytomass to the atmosphere to be 95% N, 51% P, 44% K, 52% Ca, 42% Mg, and 59% S. In addition, mineral soil dust is injected into the free atmosphere by the intense thermal convection generated by the fires.

The mineral content of smoke particles from burning biomass is related primarily to the mineral nutrients of the source vegetation, while the emission of black carbon and particulates into the atmosphere is basically a function of the fire intensity (temperature) and combustion factors such as moisture and available oxygen. Nitrogen and S are volatized in fires at temperatures as low as 600°C and then are converted to aerosols by photochemical and chemical reactions, respectively. Alka-

[1]Instituto Nacional de Pesquisas Espaciais, São José dos Campos, Brazil.
[2]Instituto de Física, University of São Paulo, São Paulo, Brazil.
[3]Fundação Cearense de Meteorologia e Recursos Hídricos, Fortaleza, Brazil.

Copyright 1996 by the American Geophysical Union.

Paper number 96JD00098.
0148-0227/96/96JD-00098$09.00

line elements (e.g., Ca and K) present in the savanna vegetation tend to be emitted to the atmosphere directly in particulate form [*Coutinho*, 1990].

Aerosols, generated by intensive burning of tropical vegetation, have been related to cloud formation [*Rogers et al.*, 1991], through its role as cloud condensation nuclei (CCN). CCN can exert a strong influence on cloud radiative parameters with indirect effects on the radiative balance of the atmosphere. In addition to these indirect effects on the radiative balance of the atmosphere, aerosols directly reflect sunlight back into space. A particularly important component of the pyrogenic aerosols is black carbon (BC), composed of elemental carbon and graphite carbon or "soot". Owing to its characteristic light absorption and scattering properties, BC can play an as yet unknown contribution to radiactive balance [*Chylek et al.*, 1984].

Large ratios of black carbon to K have been associated with the atmospheric transport of burning biomass emissions in remote oceanic areas [*Andreae*, 1983], and also in the Brazilian Amazon region [*Andreae et al.*, 1988], at the very beginning of a dry season. *Holben et al.* [1995] have recently measured a decrease in total daily insolation of 28–35% in the Amazon region, caused by the emissions from burning biomass at the peak of the dry/fire season.

This paper presents the results of different airborne aerosol measurements in the troposphere related to burning biomass, made by the Brazilian team of the U.S. NASA mission Transport and Atmospheric Chemistry Near the Equator–Atlantic (TRACE A) [*Fishman et al.*, this issue], conducted in Brazil during the second half of September 1992. This work also includes results from the 2 weeks that preceded TRACE A, when the dry/fire season for most of Brazil was close to its end. The reported data contribute to the knowledge of large-scale distributions of aerosols emitted from vegetation fires, a subject not yet properly evaluated. This paper also shows a previously unknown relation between fire detection by satellite and in situ aerosol concentrations.

Instruments and Methods

The aircraft employed in this mission was a twin-engine Embraer/Brazil EMB110 Bandeirantes, equipped with a central data acquisition system based on a PC 486 microcomputer. The aircraft is the property of the "Fundação Cearence de Meteorologia e Recursos Hídricos" (FUNCEME-Brazil) and is mainly used for cloud research purposes. It was adapted to the needs of the TRACE A mission by including the subsequently described supplementary equipment.

Real-time onboard instrumentation consisted of two laser particle counters for small and large aerosol particles, and a black carbon monitor. Small particles were measured by a condensation nuclei counter (TSI, CNC-3760) for sampling and counting small particles. This instrument uses a 5-mW laser diode as light source to detect and count small aerosol particles with diameters >0.014 μm, over the range of 0 to 10^4 particles/cm^3 (at 6% coincidence level, factory calibrated). The response time is approximately 2 s at a constant flow rate of 1.4 L per minute. Black carbon (BC) concentration was measured by an Aethalometer (Magee Sci.), a device based on the optical attenuation of a beam of light transmitted through the sample when collected on membrane filters. In order to achieve the maximum sensitivity of 17 ng/m^3 at the 1-min time base, we used an (high) air flow rate of up to 65 L per minute, provided by a dual stage air pump and low flow impedance air filters. Calibration was provided by the manufacturers. An intercomparison between absolute BC and the Aethalometer measurements for burning biomass aerosols have shown that, for these particles, the original Aethalometer calibration is acceptable (H. Cachier, personal communication, 1995).

The forward scattering spectrometer probe (FSSP) (PMS, model FSSP-100) was used to measure particles in the 0.5–8 μm size range. The FSSP results proved to be of very limited use in the characterization of the burning biomass aerosols, owing to the low counting statistics obtained in most cases. FSSP results were used in this paper only to detect the presence of clouds during the process of data reduction and interpretation.

Integration time was set to 1-min for all instruments owing to the relatively slow response time of the Aethalometer. Nonetheless, this integration time was well above the response time of the particle counters. The corresponding spatial sampling scale was about 7 km, assuming a mean aircraft speed of about 400 km/hr.

Air inlets for the Aethalometer and for the condensation nuclei counter were isokinetically tapped from a large diameter (2.5-cm radius) manifold pipe inside the aircraft, with its inlet pointing into the oncoming airstream and located just above the pilot cabin, and the outlet located near the tail. Sampling inlets were also of the isokinetic type for the FSSP, which was mounted on a pilon below one of the aircraft's wings.

Aerosols were collected simultaneously on independent Nuclepore filters for elemental analysis at the University of São Paulo by the particle-induced X ray emission (PIXE) technique [*Artaxo and Orsini*, 1987], and on Teflon filters for total mass (TM) measurements by the gravimetry method. A two-stage cascade impactor, with 50% efficiency cuttoff diameters of 1.0 μm and 0.5 μm, was also used, and its deposition surfaces were also irradiated for PIXE.

Several air pumps were installed in the aircraft to collect aerosols on the filters, with air flow rates of up to 25 L/min. Flow rates through filters and integration volumes were measured and regulated by Hasting precision mass flowmeters. Filter sampling times were typically in the range 1.5 to 3 hours. The aerosol inlets were designed to be isokinectic for typical sampling flow rate and aircraft velocity. Most of the particles were in the fine mode (<2 μm), thereby reducing the nonisokinectic sampling effects. Inlet air samplings were located in the top and bottom frontal parts of the aircraft and ahead of the propellers, in order to prevent autocontamination, and as close as possible (<1 m) from the pumps/filters booth, in order to minimize particle losses.

The aerosol filters collected during the mission flights were prepared in a laboratory clean room and sealed in containers. After sampling they were sealed again and only opened within the clean room for analysis. Blank filters were handled identically to the aerosol samples.

Ancillary measurements included geographical position and altitude of the aircraft from a Global Positioning System (GPS) (TNL-2000), external air temperature, and static pressure. The aircraft was not pressurized, thus imposing a maximum limit of 4,000 m in flight altitude. Fully equipped and with the mission team, the aircraft flew for ~5 hours at a speed of ~400 km/hr.

The missions flown were part of the NASA TRACE A experiment and were originally scheduled to be simultaneous with those of NASA's DC-8 aircraft over Brazil, for the period

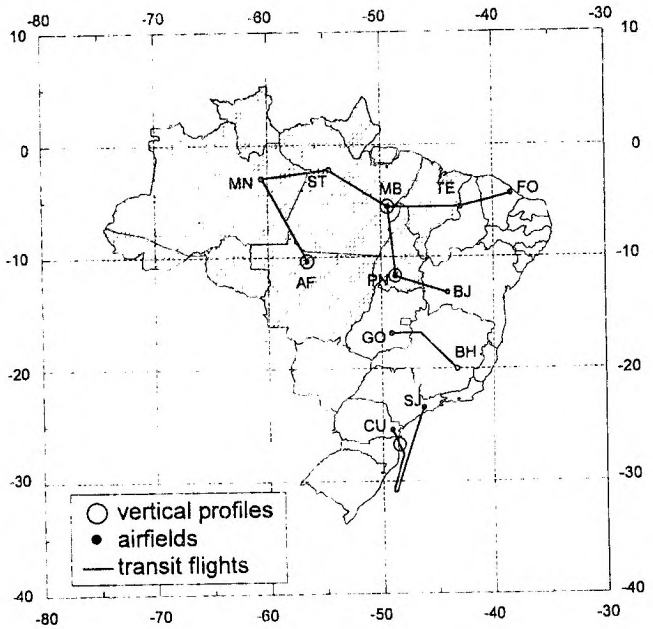

Figure 1. Flight missions for the FUNCEME aircraft during TRACE A, September 2 to 29. The abbreviations in the figure are: MN (Manaus), ST (Santarém), MB (Marabá), AF (Alta Floresta), TE (Terezina), FO (Fortaleza), PN (Porto Nacional), BJ (Bom Jesus da Lapa), GO (Goiânia), BH (Belo Horizonte), SJ (São José dos Campos), and CU (Curitiba).

of September 18–29, 1992. However, to obtain a better characterization of emissions from burning biomass, flights actually started on September 2, closer to the peak in fire activity for most of Brazil. The dry season of 1992 was relatively wet, when compared to previous years and the early start of our flights avoided the effects of the anticipation of the rainy season which followed.

Flight scenarios for the mission are depicted in Figure 1, specified in Table 1, and included several vertical profiles and level transit flights. The maximum altitude during vertical profiles was limited to ~4,000 m. Transit flight altitudes followed airway regulations in each region and were up to ~3,700 m.

Satellite image analysis was employed to detect vegetation fires in Brazil during the experiment. This was achieved daily using one afternoon image from the advanced very high resolution radiometer (AVHRR) aboard the NOAA 11 satellite, through its (thermal) channel 3 (3.55–3.93 μm). This technique, described by *Setzer and Pereira* [1991a] and *Pereira and Setzer* [1993], counts the number of pixels (picture elements of the digital satellite image) that are associated with ground fire spots. Nevertheless, it is not possible to quantitatively derive burning areas using this methodology. Independent measurements have shown that biomass fires as small as 30 m can provide saturation in the grey scale and can be counted as a single fire spot. The size of one pixel for the NOAA 11 satellite, beneath the satellite's overflight, is about 1 km^2. Satellite images were collected daily by the Instituto Nacional de Pesquisas Espaciais (INPE) satellite receiving station at Cachoeira Paulista, São Paulo, and were automatically processed. Data products were in the form of maps containing the position of individual fire spots and as statistical tables of fire spot frequencies. This information was routinely obtained during the course of the mission in order to direct flight trajectories to areas of burning biomass activities.

Results and Discussion

Forest fires detected by the AVHRR thermal channel occurred mostly in the states of Mato Grosso, Pará, Tocantins, and Maranhão. Monthly integrated counts of fire spots for the whole Brazilian Amazon region (The Brazilian Amazon is composed of the states of Acre, Amazonas, Maranhão, Mato Grosso, Pará, Roraima, and Tocantins) during dry season/1992 are shown in Table 2. The peak of this burning season was in August. Usually, the rainy season begins by mid-October in the central part of the country.

Figure 2 shows the plot of burning spots integrated for the period of September 1–10. The region where clearings and burns of tropical forests change into pasture and farming land occur is spread over the southern boundary of the tropical forest and advances northward toward its interior. A typical picture of the distribution of daily fires in this area is found in work by *Setzer and Pereira* [1991a]. As shown in Table 2, ~123,000 fire spots were detected by the AVHRR during the June–September period in the Brazilian Amazon, or ~74% of the corresponding total of ~166,000 fire spots for all of Brazil. However, it should be pointed out that most fires in the Brazilian Amazon refer to the reburn of forests cleared in previous

Table 1. Mission Flights Data

Flight Name	Date	Itinerary	Description
FOTE02	September 2	Fortaleza-Terezina	Transit flight
TEMB02	September 2	Terezina-Marabá	Transit flight
MBMB03	September 3	Marabá-Marabá	Vertical profile
MBST04	September 4	Marabá-Santarém	Transit flight
STMN04	September 4	Santarém-Manaus	Transit flight
MNAF05	September 5	Manaus-Alta Floresta	Transit flight
AFAF10	September 10	Alta Floresta-Alta Floresta	Vertical profile
SJPA24	September 24	S. J. Campos-P. Alegre	Outflow intercept
CUCU24	September 24	Barra Velha-Curitiba	Vertical profile
GOBH26	September 26	Goiania-Belo Horizonte	Along outflow
BJPN27	September 27	Bom Jesus-Porto Nacional	Transit flight
PNPN28	September 28	P. Nacional-P. Nacional	Vertical profile
PNPN29	September 29	P. Nacional-P. Nacional	Vertical profile
MBMB29	September 29	Marabá-Marabá	Vertical profile

Average transit flight altitude is 2162 ± 561 m.
Typical vertical profile altitude range is 500 to 4000 m.

Table 2. Burning Spots in Brazilian Amazon States for the Dry Season of 1992, Derived From the AVHRR/NOAA Satellite Thermal Sensor

Month, 1992	Acre	Amazonas	Maranhão	Mato Grosso	Pará	Roraima	Tocantins	Total, Month
June	0	15	473	1,416	200	24	1,376	3,504
July	0	40	1,565	5,551	1,855	145	2,812	11,968
August	183	565	6,438	20,262	18,546	3,422	11,970	61,386
September	36	331	7,863	12,050	8,512	2,834	14,347	45,973
Total/state	219	951	16,339	39,279	29,113	6,425	30,505	122,831

*Total for Brazil: 166,411 fire counts (73.8%).
This represents 73% of the total burning spots observed for Brazil.

years and to the conversion to savanna. In other parts of the country, fires are mostly associated with pasture renewal, preharvesting of sugar cane, and miscellaneous agricultural practices.

In order to compare aerosol and black carbon data with the fire spots detected by the (satellite) AVHRR, the following procedure was devised: fire spots were first integrated over a fixed time interval before each flight date, for several nominal circles of investigation ranging in radius from 50 to 1,000 km. These circles were centered close to the geographic location of each of the vertical profile flights. In the case of transit flights their center was halfway between the two airfields used in the corresponding flight. A 3-day integration time was chosen based on results of isentropic back-trajectories calculations by S. Bachmeier (personal communication, 1994). This procedure allows for the study of the spatial variability of the influence of AVHRR fire spots on black carbon and small aerosols. Results of the integrated AVHRR fire spots for each nominal radius are presented in Table 3.

Figure 3a and 3b shows the minimum and maximum range

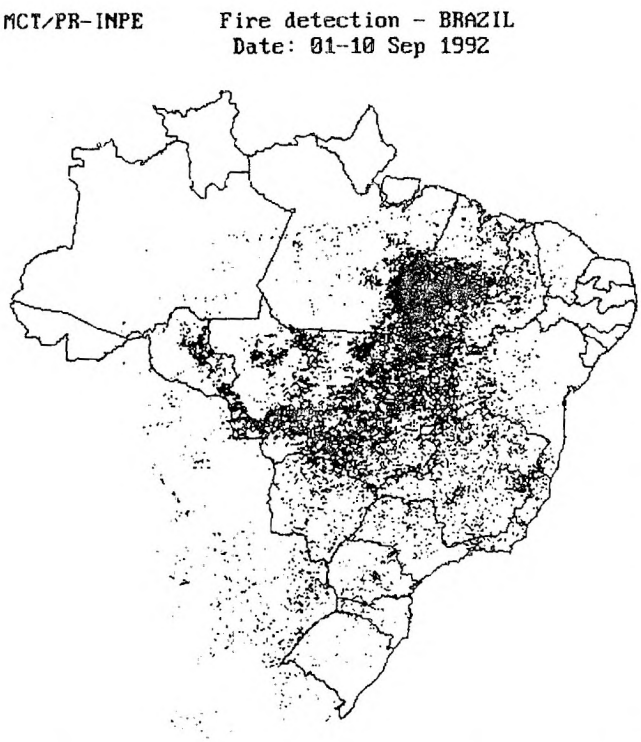

Figure 2. AVHRR/NOAA satellite biomass burning spots distribution for the period of September 1 to 10, 1992.

of concentrations for black carbon and small particles considering all profile flights. The highest black carbon, reaching an absolute peak of ~12,000 ng/m^3, was obtained over Marabá, on September 3 (MBMB03). This peak coincided with the largest number of AVHRR satellite fire spots detected for the whole experiment and also with the highest overall profile of small particles for the experiment, when a peak of ~16,000 particles/cm^3 was obtained. The mean black carbon concentration found during this vertical profile (7,400 ng/m^3) was comparable to values reported at ground level for large cities like New York (4,200–13,300 ng/m^3), Los Angeles (400–13,100 ng/m^3), and Paris (1,600–10,200 ng/m^3), by *Hamilton and Mansfield* [1991].

The vertical profile for black carbon and small particles with the lowest values was obtained over Porto Nacional, on September 27 (PNPN27), by the end of the burning season, when the early onset of rains for the season prevented farmers from burning additional areas; this is in contrast with the profile of the highest concentrations measured, which were less by nearly 1 order of magnitude. Mean black carbon found during this vertical profile (900 ng/m^3) was comparable to values found at ground level for an average of 1,300 ng/m^3 for 20 rural sites in the United States [*Shah et al.*, 1986].

The curves for maximum vertical concentration profiles of black carbon and small aerosols (Figure 3) reach their peak values at altitudes around 2,200 m above sea level; and similar features were observed in all other flights over regions of burning biomass. The altitudes of higher concentrations were

Table 3. Three-Day Integrated Fire Spots Counted Inside Several Nominal Circle of Investigations for Each Flight

Flight	50 km	250 km	500 km	1000 km	Total
FOTE02	0*	25	259	5124	11665
TEMB02	52*	1310	4638	8273	11665
MBST04	7*	256	3259	13444	20885
STMN04	2*	13	33	2788	20885
MAAF05	1*	10	83	4278	16391
PNMB29	15*	400	2496	8439	10816
GOBH26	6*	55	407	1971	6262
BJPN27	6*	358	1021	2394	4299
SJPA24	0*	10	64	415	3297
PNPN27	37	498	1904	8729	10816
PNPN28	52	615	2080	7075	11921
AFAF10	191	924	3640	12208	14710
MBMB03	659	3953	8803	13650	17104
MBMB29	90	701	1686	6917	10816
CUCU24	2	10	126	665	3297

*Circle of investigation too small.
The column corresponding to "Total" gives the total fire counts integrated over the whole Brazilian area (8,550,000 km^2).

between 2,000 m and 3,000 m, with only minute levels measured close to 4,000 m. Comparison with air temperature profiles showed that the concentration peaks were located between small temperature inversions or above a slight increase in the gradient in the temperature profiles. Such stable layers are actually expected in the dry/fire season when stable anticyclone tropospheric circulation prevails in the region. This condition is well characterized in Figure 4 and shows the temperature profile for September 29 over Marabá with two inversion layers at ~2,000 m and ~3,000 m, and the corresponding peaks in the black carbon and small particles profiles concentrations. In this case the upper inversion layer is the reason for the trapping of aerosols up to the level of ~3,000 m, and for the high levels of black carbon between the two inversion layers. This vertical profile also shows a considerable enhancement of small particles relative to the black carbon concentrations at low altitudes (below about 1,300 m). Although the aircraft avoided fire plumes during low altitude flights, the small particle enhancement at low levels was probably linked to fresh smoke plumes, with their higher content of small organic particles and volatiles. The black carbon to total mass ratio was 1.3%, one of the lowest found in Table 4.

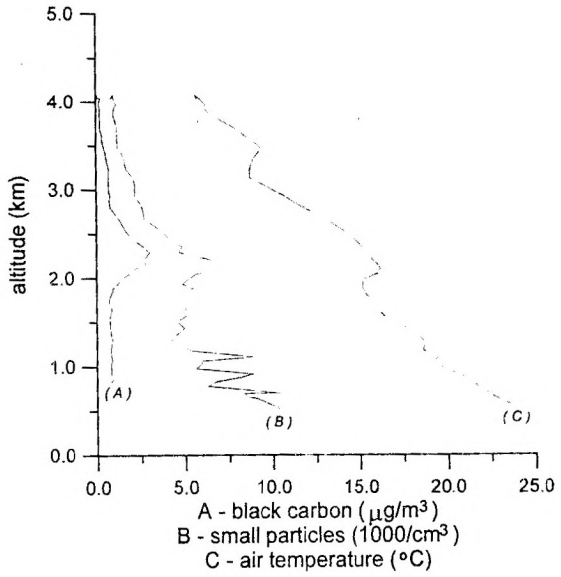

Figure 4. Vertical profile near Marabá on September 29 (MBMB29).

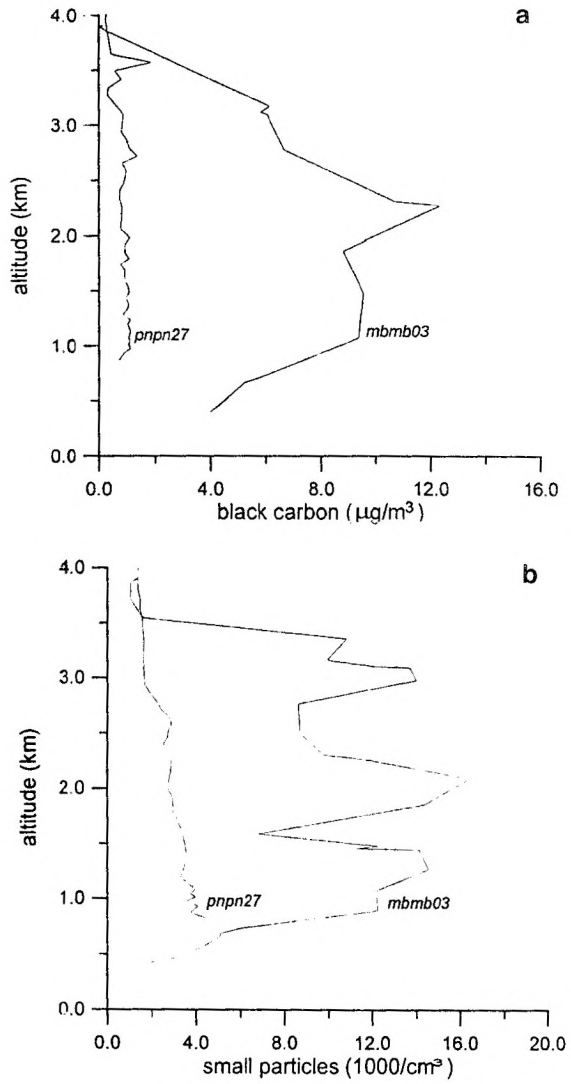

Figure 3 Range of concentration profiles for (a) black carbon and (b) small particles.

The overall mean results for total aerosol mass concentration, for small particles, and for black carbon are shown in Table 4, along with the ratio between total mass concentration and black carbon. The maximum total mass, measured by gravimetry, was found for the MBMB03 vertical profile (200 $\mu g/m^3$) and was about 1 order of magnitude larger than for the other flights. During this flight about 660 fire spots were counted in a 50-km radius circle of investigation; it was the largest value found for the whole mission. Fire spot count were also maximum for larger circles of investigations, but not for the total counts found for the entire country (~17,000). Mean maximum black carbon was ~7,400 ng/m^3 (absolute maximum of 12,000 ng/m^3 at about 2,400 m). The small particles load was also the highest during this flight (~9,900 particles/cm^3), yet with a markedly different vertical profile of concentrations. Although only a few fires of moderate extension could be seen from the airplane cabin during this flight, the visibility was quite low, probably as a consequence of smoke transport from neighboring regions.

In contrast to the high concentration peaks, the smallest mean for black carbon concentrations (67 ng/m^3), and for small particles (677 particles/cm^3), were obtained at the beginning of the mission for flight FOTE02, from Fortaleza to Terezina and typify the ocean air background for particulates. The coastal region of Fortaleza is influenced by the westward air circulation driven by the quasi-permanent high pressure center over the tropical South Atlantic Ocean, which brings relatively clean air from the Atlantic ocean (total mass concentration of only 17.2 $\mu g/m^3$). Five-day isentropic backtrajectories were calculated and evidenced an air mass flow from the ocean intercepting the flight path after a short transit over land. As the flight proceeded toward Marabá (flight TEMB02, same day) back-trajectories calculations showed increased land influence which lead to a drastic growth in black carbon of about 1 order of magnitude. The ratios between black carbon and total mass concentration shown in Table 4 evidence this land influence.

The black carbon content in the total mass concentration of

Table 4. Total Aerosol Mass Concentration, Small Aerosol Loads and Black Carbon Concentration for Each Mission Flights

Flight	Height, m	Black Carbon (*BC*), ng/m^3	Small Particles, #/cm^3	Total Mass (*TM*), μg/m^3	BC/TM, Percent
FOTE02	2600	67	***	17.18	0.4
TEMB02	2586	491	***	41.67	1.2
MBST04	1196	419	2546	39.68	1.1
STMN04	2244	1710	4343	32.67	5.2
MAAF05	1706	865	1500	32.49	2.7
PNMB29	2365	1408	3863	111.1	1.3
GOBH26	1345	722	3000	21.30	3.4
BJPN27	2770	554	2559	15.83	3.5
SJPA24	2650	667	2568	25.99	2.6
PNPN27	v.p.	899	27118	10.05	8.9
PNPN28	v.p.	697	2817	15.83	4.4
AFAF10	v.p.	2018	3764	30.46	6.6
MBMB03	v.p.	7382	9908	206.7	3.6
MBMB29	v.p.	921	4422	10.99	8.4
CUCU24	v.p.	999	4743	23.30	4.3

Note: v.p. is vertical profiles.

aerosols particles was found to be highly variable, ranging from 0.4 to 8.4%. These values are low when compared to the 4 to 40% estimated by *Patterson and McMahon* [1984] or of 18% by *Crutzen and Andreae* [1990]. The correlation coefficient between black carbon and total aerosol mass load for all data of all missions was only 0.32 (0.26 confidence level). This is explained by the fact that black carbon represents on average only about 5% of the total mass of the aerosols, according to the data in Table 4 for flights performed in burning biomass areas. On the other hand, black carbon had a significantly higher correlation coefficient of 0.69 (0.01 confidence level) with small aerosol particle counts. This latter result was expected since black carbon particles are mostly submicron. The submicron particles are responsible for the majority of the counts in the condensation nuclei counter (CNC).

Correlations between small aerosol particles, black carbon, and total mass concentration with fire spots are graphically shown in Figure 5, for several nominal ranges of investigation. We have employed the r-Spearman nonparametric statistics to estimate these correlations. This test measures the degree of agreement or disagreement between two variables based on the ranks of data rather than the values themselves, and does not depend on the type of statistical distribution. Figure 5 comprises only vertical profile flights in order to consider the vertical changes in concentration. As expected, results for black carbon, small particles, and total mass are well correlated with fire spots counted within the 50 to 250 km range of investigation because of the ubiquitous burning biomass sources in this area. A steep decrease in the correlation coefficients after 250 km, marks the limit of influence of burnings of biomass on the local concentration of pyrogenic emissions. A similar relation between satellite fire spots and burning biomass emissions, but for the case of ozone, has been previously reported [*Setzer et al.*, 1993].

Figure 6 shows the plot of concentrations of black carbon versus fire spots integrated for the 50-km circle of investigation for all the vertical profiles within Brazilian Amazon region. The linear regression on these points is excellent, with $r > 0.99$, which suggests the possibility of estimating local concentrations of black carbon and other aerosol fire emissions in the atmosphere by using satellite data. The relationship between fire spot counts (FC) and black carbon (BC) is given by:

$$\mathrm{BC(ng/m^3)} = 10.9 \pm 0.5 \times \mathrm{FC} + 174. \pm 265.(r = 0.99). \quad (1)$$

In order to evaluate the weight of the one point removed from the rest of the distribution (MBMB03) on this regression coefficient, a second linear regression line (dashed line) was also drawn not including this point in the calculations. As can be seen from this figure, this second line also shows a good linear regression coefficient (>0.99) but with a minor change in slope. This indicates that the good linear regression coefficients obtained are not an artifact caused by this more distant data point. The linear regressions obtained for total aerosol mass (TM) and for small aerosol particles (SP) counted by the CNC displayed the same behavior, and are, respectively, given by

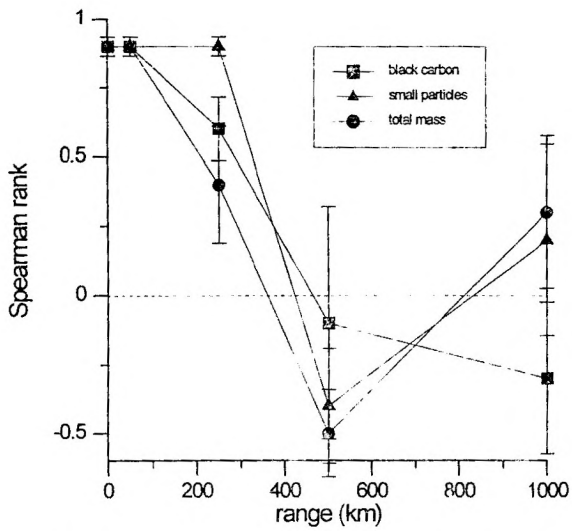

Figure 5. Spearman rank correlation coefficient versus range of circles of investigations for black carbon, total mass concentration; and small particles. The rapid drop of correlations at about 250–500 km suggests a limit for the influence of burnings on local aerosol characteristics.

$$TM(\mu g/m^3) = 0.32 \pm 0.03 \times FC + 12. \pm 15.(r = 0.98), \quad (2)$$

and

$$SP(1/cm^3) = 11. \pm 1. \times FC + 2433. \pm 748.(r = 0.95). \quad (3)$$

These data points, however, and the corresponding regression lines, are not shown in order to avoid cluttering this figure with an excess of information.

Elemental composition and associated standard deviations found for aerosols concentrations in the Nuclepore filters are shown in Table 5. Owing to the long collection time of a few hours for aerosols on filters, the results presented are the mean values for the entire flight. Missing values are reported as asterisks in this table. Major soil derived elements such as Al and Si ranged from 120 to 1000 ng/m^3 for Al and from 500 to 5,200 ng/m^3 for Si. Potassium, which has been linked to the burning biomass [*Andreae et al.*, 1988; *Crutzen and Andreae*, 1990], ranged from 100 to 7,700 ng/m^3. Other biomass associated elements such as S and Ca ranged from 360 to 3,800 ng/m^3 and from 110 to 11,100 ng/m^3, respectively.

Potassium and S presented very good correlations (r-Spearman) against black carbon, as seen in Table 6. Furthermore, the ratio between K and black carbon was fairly constant between 0.43 and 0.75, with only one case above 1 (MBMB03 = 1.04), considering flights performed in regions of burning biomass. This is consistent with the pyrogenic origin of these two elements. Nevertheless, the flight which presented the greatest maritime influence also presented the greatest K:BC (FOTE02 with 1.5). Correlations between K and total mass concentration of aerosols (0.46) was much lower, with high K:TM values found for flights occurring in high burning of biomass areas such as MBMB03 (0.037). The correlations for all other trace elements with black carbon were low and statistically nonsignificant in this work. Potassium and S concentrations in the small particles were also statistically significant and, as expected, presented lower correlation coefficients when compared to the black carbon correlations. Iron was found to

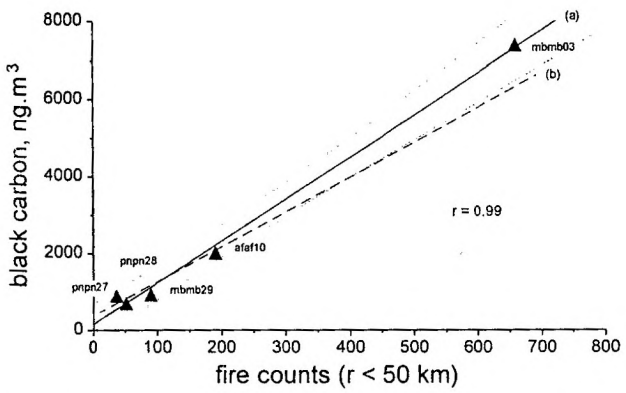

Figure 6. AVHRR/NOAA fire spot counts for 50-km radius circle of investigation versus black carbon for the vertical profile flights. The correlation coefficient is high and the adjusted straight line (solid line) through the points is shown along with the 95% confidence level (dotted lines). A second regression line (dashed line) is also adjusted through the points but excluding the very high MBMB03 data point.

Table 5. Aerosol Elemental Composition Determined by the PIXE Method

FLIGHT	Al	Si	S	Cl	K	Ca	Ti	Mn	Fe	Cu	Zn	As	Br	Sr
FCTE02	322 (42)	860 (120)	362 (56)	977 (54)	100.8 (7.7)	237 (42)	26.5 (3.2)	7.2 (7.2)	82.8 (6.8)	2.73 (0.75)	8.6 (1.7)	***	***	***
TEMB02	470 (37)	1290 (110)	749 (54)	258 (18)	555 (21)	847 (53)	43.9 (3.4)	14 (1.4)	135 (8.5)	3.46 (0.68)	3.77 (0.8)	1.77	***	5.7
MBST04	123 (84)	2430 (180)	577 (75)	32 (16)	266 (15)	218 (42)	14.1 (3.3)	8.2 (1.5)	90.8 (7.4)	1.96 (0.77)	13.1 (1.5)	***	12.4 (7.0)	***
SITMN04	543 (35)	1190 (120)	1019 (63)	***	737 (27)	260 (28)	32.5 (2.9)	6.1 (1.0)	100.0 (6.8)	2.47 (0.61)	7.0 (0.8)	1.21 (0.5)	***	***
MAAF05	430 (49)	686 (88)	1040 (54)	74 (16)	568 (16)	477 (31)	26.4 (3.8)	12.0 (1.2)	114.0 (5.4)	6.92 (0.85)	11.0 (0.9)	1.6 (0.7)	12.3 (5.2)	5.8 (2.9)
PNMB29	207 (28)	503 (99)	1221 (77)	***	760 (28)	199 (33)	22.1 (2.7)	5.9 (1.2)	173.5 (8.6)	9.9 (1.5)	7.7 (1.1)	2.45 (0.75)	***	***
GOBH26	***	495 (90)	510 (51)	***	321 (12)	***	***	4.4 (1.2)	55.0 (4.4)	1.75 (0.46)	4.49 (0.75)	12.8 (2.0)	***	***
BJPN27	173 (18)	498 (64)	664 (44)	***	409 (15)	275 (22)	19 (1.8)	6.2 (0.8)	86.6 (4.8)	2.70 (0.44)	4.57 (0.65)	***	***	***
SJPA24	144.2 (7.7)	315 (38)	950 (73)	***	403 (23)	48.9 (5.9)	26.8 (2.9)	***	159 (6.5)	8.0 (2.7)	9 (2)	***	***	***
PNPN28	147 (19)	***	556 (46)	***	311 (12)	112 (30)	21.0 (2.6)	4.5 (0.8)	73.8 (4.7)	2.61 (0.49)	5.1 (0.7)	1.3 (0.8)	***	3.3 (1.7)
AFAF10	123 (27)	486 (73)	1217 (66)	***	965 (35)	381 (28)	18.8 (2.3)	5.2 (1.1)	87.2 (5.2)	***	6.94 (0.81)	***	11.2 (5.0)	5.7 (1.8)
MBMB03	997 (84)	5160 (330)	3760 (220)	2070 (110)	7690 (390)	1080 (560)	164 (11)	251 (14)	1245 (65)	10.0 (2.4)	29.7 (3.8)	***	44 (12)	89 (14)
MBMB29	315 (55)	630 (200)	887 (89)	***	494 (20)	149 (48)	***	9.4 (2.5)	113.5 (8.0)	6.2 (1.1)	8.6 (1.2)	***	***	***
CUCU24	596 (45)	1680 (120)	944 (62)	***	480 (18)	265 (29)	25.4 (2.6)	9.3 (1.1)	145 (7.7)	3.62 (0.63)	8.1 (0.9)	***	***	***

The standard deviations for each measurement are shown within parentheses. Concentrations below the detection limits for the PIXE analysis are represented by asterisks. Aerosol elemental composition is measured in nanograms per cubic meter.

Table 6. Correlation Coefficients (r-Spearman) Between the Elemental Composition of Table 5, and Black Carbon Concentrations, Number of Small Aerosol, and Total Aerosol Mass Loads of Table 4

Element	Rank
Black Carbon	
K	0.80 (0.006)
S	0.80 (0.009)
Small Particles	
K	0.56 (0.06)
S	0.38 (0.21)
Fe	0.34 (0.26)
Total Mass	
Fe	0.55 (0.06)
S	0.52 (0.07)
K	0.46 (0.11)
Si	0.31 (0.29)
Ca	0.31 (0.30)

Confidence levels are in parentheses. Only trace elements with not more than one missing value were considered in this analysis.

be important in the small particles, indicating a mixed influence of soil dust uplift in the submicrometer burning biomass emissions. The total mass presented a more complex matrix of correlations that included soil tracers such as Si and Fe, along with the biogenic S, K, and Ca, at statistically significant levels.

Mineral content in the burning biomass emissions is directly related to the rate of heat release of the biomass during the flaming phase. Sulfur, for example, is easily volatilized in a fire at relatively low temperature (above 600°C), while the alkaline elements K and Ca are lost primarily in particulate form [*Coutinho*, 1990]. Furthermore, as summarized by *Coutinho* [1990] for a savanna fire in southern Brazil, a negative correlation exists between the Ca export to the atmosphere and the degree of combustion of the vegetation. As for the carbonaceous particulates, the rate of emission is favored at low-temperature fires (<800°C) and oxygen deficiency [*Ward*, 1990]. The high enrichment of Ca with respect to total mass and black carbon (0.54% and 150%, respectively) in the MBMB03 vertical profile flight may be linked to this low degree of combustion (low temperatures) of nearby fires. This hypothesis is further supported by the fact that the K to black carbon ratio (1.0) was also high for this flight.

Both the K:TM and Ca:TM ratios decreased at the end of the TRACE A experiment for the same site as evidenced by the comparison of flights MBMB03 on September 3 during the maximum burning biomass activity and of MBMB29 on September 29 after the early onset of rains for the season.

Figure 7 depicts the results for black carbon and small particles during flight SJPA24, from São José dos Campos to Porto Alegre. This flight was performed in an attempt to intercept the burning biomass aerosols from central Brazil that outflowed to the Atlantic Ocean. This outflow follows the major tropospheric circulation pattern for South America which is linked to a static subtropical high in the South Atlantic. The transit flight shows a simultaneous increase of elemental carbon and small particles between 1115 and 1200 LT, when the airplane was flying off the São Paulo–Santa Catarina coast at about 2.6 km altitude. A cold front was located north of Rio Grande do Sul state which favored the eastward outflowing circulation toward the Atlantic Ocean in the warm branch of this front. The percentage of black carbon with respect to the total mass concentration (2.6%) was lower than values found for flights performed in the burning biomass regions (MBMB03: 3.6%, AFAF10: 6.6%), but much larger than for the flight under strong maritime influence (FOTE02: 0.4%). The ratio between K and black carbon (0.6) was comparable to values linked to concentrations found in the Brazilian Amazon during the burning season. Nevertheless, the sulfur-to-potassium ratio was 2.3, close to the ratio in the urban environment of a large industrial city such as São Paulo (2.9, measured at ground level). compared to all other flights (around 1.5), except for the maritime flight FOTE02 (3.6). In the case of SJPA24, which was also flown over the sea, this excess sulfur could be linked to the sulfate from oxidation of marine dimethylsulfide (DMS). Although the increase in black carbon and small aerosols occurred in a broad area, extending further south from the major urban centers of São Paulo and Rio de Janeiro, the air masses that moved off the continent may have been contaminated by urban pollution produced in these large cities during the previous day and transported to our area during the previous night. *Anderson et al.* [this issue] have also detected haze layers related to this outflow on more than one occasion by the NASA DC-8 aircraft flights during TRACE A. Their results show the presence of these low-level haze layers at about 2 to 5 km. A vertical profile flight shown in Figure 8 (CUCU24) was conducted at the coast line of Santa Catarina, in an area free of local urban pollution, in order to characterize this outflow. Our result is comparable with *Anderson et al.* [this issue] and his collaborators, with a broad enhancement in black carbon and small particles extending from an altitude of about 1.5 to 3.0 km.

Results of the deposition filters in the two-stage cascade impactor suggest a relation between the elemental composition of the aerosols in the fine (<1 μm) and coarse modes. Figure 9a shows the relative mass concentration (in percentage) between the two stages of the impactor for all samples. Figure 9b and 9c refer to vertical profiles with high and reduced burning of biomass, respectively, during MBMB03 and PNPN28. Primary elements associated with soil dust (Al, Si, Mn, Fe, Ni) prevailed in the coarse mode aerosols (>1 μm).

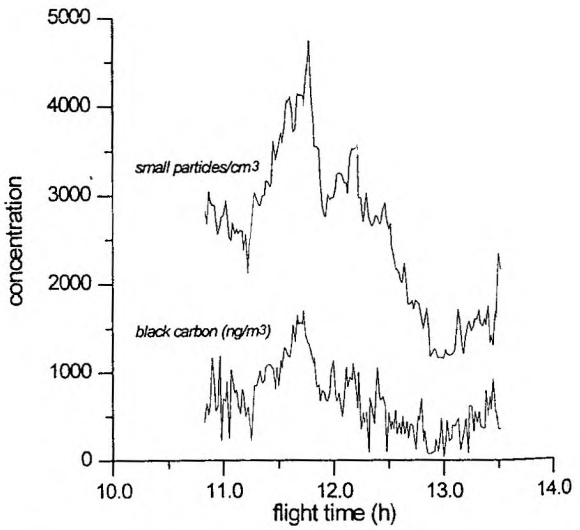

Figure 7. Small aerosols and black carbon during transit flight from São José dos Campos to Porto Alegre on September 24 (SJPA24). This flight crossed the continental outflow of pyrogenic emissions to the Atlantic ocean.

The fine mode aerosols were mostly enriched in S, K, Br, and Rb, which are tracers normally associated with burning biomass. This pattern was typical of high concentrations of particulate matter in the troposphere and high counts of fire spots, as in the MBMB03 profile. Calcium and Fe, although with distinct sources in the pyrogenic emissions, are also associated with the coarse fractions of the aerosols, which explain their positive correlation with the total mass loads, but not the correlation between Fe and small particles in Table 6.

Conclusions

As viewed by AVHRR fire spots counts during the mission, the region where clearings and burns occur of tropical forests which change into pasture and farming land, is spread over the southern boundary of the tropical forest and advances northward toward its interior. The concentrations found for black carbon was 12,000 ng/m^3 and for small particles was 16,000 particles/cm^3, comparable to values reported for large urban centers. The maximum concentration of black carbon and small particles coincided with the largest number of fire spots. The good correlation between black carbon and the integrated fire spot counts by AVHRR indicates a new, viable approach to estimate emissions based on satellite images. Linear regression for a circle of investigation with radius of 50 km yield the following concentration for black carbon as a function of fire spot counts (FC) for vertical flights in biomass burning areas: $BC(ng/m^3) = 10.9 \pm 0.5 \times FC + 174. \pm 265.$ ($r > 0.99$). Small aerosol particles (SP) also presented this good linear regression with fire counts: $SP(1/cm^3) = 11. \pm 1. \times FC + 2433. \pm 748$ ($r = 0.95$). For total aerosol mass (TM), the relation found was $TM(\mu g/m^3) = 0.32 \pm 0.03 \times FC + 12. \pm 15$ ($r = 0.98$). Small aerosol particles, black carbon, and total mass concentrations appear to be related to distance and show a strong decrease in correlation with satellite fire spots at about 250–500 km, and mark the limit of influence of burning biomass on the local concentration of particulate fire emissions.

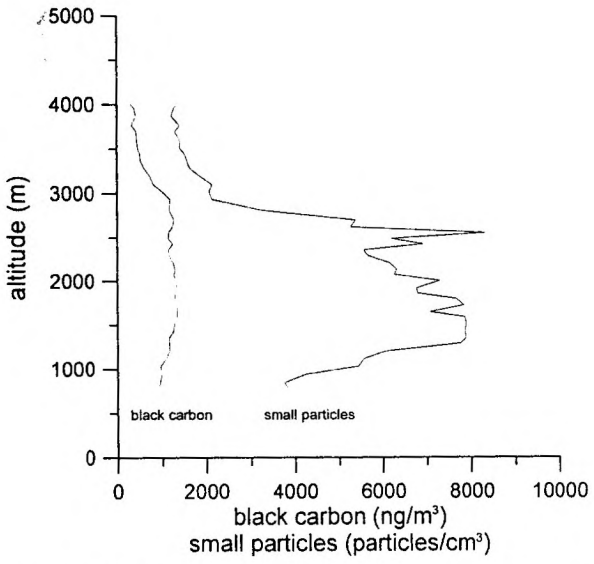

Figure 8. Vertical concentration profile of black carbon and submicrometer particles in the continental outflow of the pyrogenic aerosols to the Atlantic Ocean. This flight was conducted at the coastline of Santa Catarina on September 24 (CUCU24).

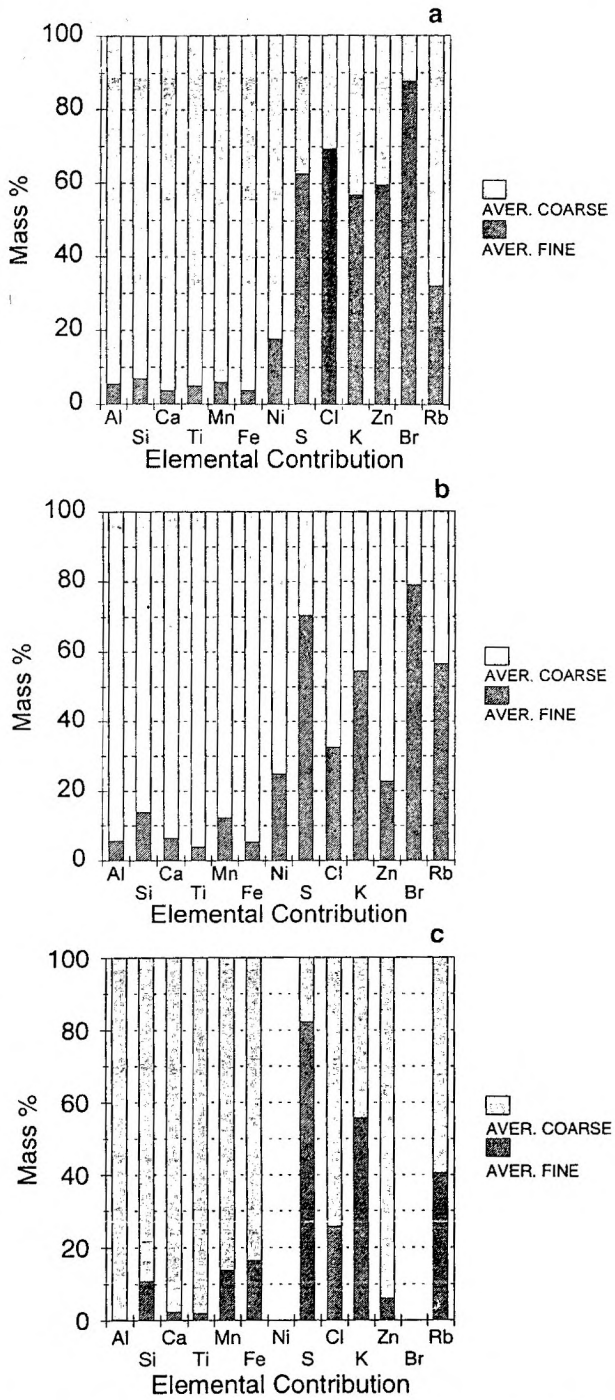

Figure 9. Relative mass concentration in percentage of total mass between the two stages of the two-stage cascade impactor. (a) All flights; (b) MBMB03; and (c) PNPN28.

The atmospheric differences between the period of high burning of biomass at the beginning of the mission (September 3), and 26 days later for the same site, just after the arrival of rains, was remarkable. Total mass concentration of aerosol decreased by more than 1 order of magnitude (~20); black carbon decreased by a factor of 8, while small particles decreased by a factor of 2.

The content of black carbon in the aerosol particles was found to be highly variable, ranging from 1.1 to 8.4% of the total aerosol mass for flights performed in regions of biomass

fires. This ratio for maritime air was much lower (0.4%). Potassium and S presented good correlation coefficients against black carbon. Furthermore, the ratio between K and black carbon was fairly constant between 0.4 and 0.7 in the burning biomass areas. Iron, Si, and Ca, along with the S and K, showed significant correlation coefficients with total mass loads, indicating a mixed influence of soil dust uplift and burning biomass in the pyrogenic emissions. All other trace elements showed nonmeaningful correlations with black carbon, small particles and/or total mass. Primary elements associated with soil dust (Al, Si, Mn, Fe, Ni) prevailed in the coarse aerosol mode (>1 μm). The fine mode aerosols were enriched in S, K, Br, and Rb, which are tracers normally associated with the burning of biomass.

Acknowledgments. The authors are thankful to NASA, which through the TRACE A experiment and its Brazilian coordinator V. W. J. H. Kirchhoff (INPE), supported a significant part of this work. Our thanks go to two reviewers for their useful and constructive comments on the original manuscript. We also thank: FUNCEME for the loan of its research aircraft used in this work; S. Bachmeier from NASA/Langley for the back-trajectory analyses; Marcelo Sampaio and Domingos Sardella from INPE for their help with the instrument setup and calibration, and Merritt Stevenson, also from INPE, for his help with the English revision. We acknowledge grants 90/2950 from FAPESP, 300914/80-6 from CNPq, and contract CT1-CT92-0082 from CEC-DGSRD.

References

Anderson, E. A., W. B. Grant, G. L. Gregory, E. V. Browell, J. E. Collins Jr, G. W. Sachse, D. R. Bagwell, C. H. Hudgins, and N. J. Blake. Aerosols from biomass burning over the tropical South Atlantic region: Distribution and impacts, *J. Geophys. Res.*, this issue.

Andreae, M. O., Soot carbon and excess fine potassium: Long-range transport of combustion derived aerosols, *Science*, *220*, 1148–1151, 1983.

Andreae, M. O., et al., Biomass-burning emission and associated haze layers over Amazonia, *J. Geophys. Res.*, *93*(D2), 1509–1527, 1988.

Artaxo, P., and C. Orsini, PIXE and receptor models applied to remote aerosol source apportionment in Brazil, *Nucl. Instrum. Methods Phys. Res.*, *B22*, 259–263, 1987.

Artaxo, P., H. Storms, F. Bruynseels, R. Van Grieken, and W. Maenhaut, Composition and sources of aerosols from the Amazon basin, *J. Geophys. Res.*, *93*, 1605–1615, 1988.

Artaxo, P., W. Maenahut, H. Storms, and R. Van Grieken, Aerosol characteristics and sources for the Amazon Basin during the wet season, *J. Geophys. Res.*, *95*, 16,971–16,985, 1990.

Artaxo, P., M. Yamasoe, J. V. Martins, S. Kocinas, S. Carvalho, and W. Maenhaut, Case study of atmospheric measurements in Brazil: Aerosol emissions from Amazon Basin Biomass Burning, in *Fire in the Environment: The Ecological, Atmospheric, and Climatic Importance of Vegetation Fires*, edited by P. J. Crutzen and J. G. Goldammer, pp. 139–158, John Wiley, New York, 1993a.

Artaxo, P., F. Gerab, and M. L. C. Rabello, Elemental composition of aerosol particles for two background monitoring stations in the Amazon basin during the wet season, *J. Nucl. Instrum. Methods Phys. Res.*, *B75*, 277–281, 1993b.

Artaxo, P., F. Gerab, M. A. Yamasoe, and J. V. Martins, Fine mode aerosol composition in three long-term atmospheric monitoring stations in the Amazon Basin, *J. Geophys. Res.*, *99*(D11), 22,857–22,868, 1994.

Chylek, P., V. Ramaswamy, and V. Srivastava, Graphitic carbon content of aerosols, clouds and snow, and its climatic implications, *Sci. Total Environ.*, *36*, 117–120, 1984.

Coutinho, L. M., Fire in the ecology of the Brazilian Cerrado in *Fire in the Tropical Biota*, edited by J. G. Goldammer, pp. 82–105, Springer-Verlag, New York, 1990.

Crutzen, P. J., and M. O. Andreae, Biomass burning in the tropics: Impact on atmospheric chemistry and biogeochemical cycles, *Science*, *250*, 1669–1677, 1990.

Fearnside, P. M., Greenhouse gas contributions from deforestation in Brazilian Amazonia, in *Global Biomass Burning*, edited by J. S. Levine, pp. 92–105, MIT Press, Cambridge, Mass., 1991.

Hamilton, R. S., and T. A. Mansfield, Airborne particulate elemental carbon: Its sources, transport and contribution to dark smoke and soiling, *Atmos. Environ.*, *25A*, 715–723, 1991.

Fishman, J., J. Hoell, R. D. Bendura, V. W. J. H. Kirchoff, and R. J. McNeal, The NASA GTE TRACE A experiment (September–October 1992): Overview, *J. Geophys. Res.*, this issue.

Holben, B. N., A. W. Setzer, T. F. Eck, M. C. Pereira, and I. Slutsker, Effect of dry-season biomass burning on Amazon Basin aerosol concentrations and optical properties, 1992–1994, *J. Geophys. Res.*, *101*, 19,465–19,481, 1996.

Kaufman, Y. J., A. Setzer, D. Ward, D. Tanré, B. N. Holben, P. Menzel, M. C. Pereira, and R. Rasmussen, Biomass burning airborne and space borne experiment in the Amazon (BASE-A), *J. Geophys. Res.*, *97*, 14,581–14,599, 1992

Levine, J., Global biomass burning: atmospheric, climatic and biospheric implications, *EOS Trans. AGU*, *71*(37), 1075–1077, 1990.

Patterson, E. M., and C. K. MacMahon, Absorption characteristics of Forest Fire particulate matter, *Atmos. Environ.*, *18*, 2541–2555, 1984.

Pereira, M. C., and A. W. Setzer, Spectral characteristics of deforestation fires in NOAA/AVHRR images, *Int. J. Remote Sens.*, *14*(3), 583–597, 1993.

Rogers, C. F., J. G. Hudson, B. Zielinska, R. L. Tanner, J. Hallet, and J. G. Watson, Cloud condensation nuclei from biomass burning, in *Global Biomass Burning*, edited by J. S. Levine, pp. 431–438, MIT Press, Cambridge, Mass., 1991.

Setzer, A. W., and M. C. Pereira, Amazonia Biomass Burning in 1987 and an estimate of their tropospheric emissions, *Ambio*, *20*, 19–22, 1991a.

Setzer, A. W., and M. C. Pereira, Operational detection of fires in Brazil with NOAA/AVHRR, Proc. *Int. Symp. Remote Sens. Environ.*, pp. 469–482, Rio de Janeiro, RJ, May 27–31, 1991b.

Setzer, A. W., V. W. J. Kirchhoff, and M. C. Pereira, Ozone concentrations in the Brazilian Amazonia during BASE-A, in *Global Biomass Burning*, edited by J. S. Levine, pp. 112–114, MIT Press, Cambridge, Mass., 1993.

Shah, J. J., R. L. Johnson, E. K. Heyerdahl, and J. Huntzicker, Carbonaceous aerosols at urban and rural sites in the United States, *J. Air Pollut. Control Assoc.*, *36*, 254–257, 1986.

Ward, D. E., Factors influencing the emissions of gases and particulate matter from biomass burning, in *Fire in the Tropical Biota*, *Ecological Studies 84*, edited by J. G. Goldammer, pp. 418–436, Spring-Verlag, New York, 1990.

Ward, D. E., and C. C. Hardy, Smoke emissions from wildland fires, *Environ. Int.*, *17*, 117–134, 1991.

Ward, D. E., R. A. Sussot, J. B. Kauffman, R. E. Babbitt, D. L. Cummings, B. Dias, B. N. Holben, Y. J. Kaufman, R. A. Rasmussen, and A. W. Setzer, Smoke and fire characteristics for cerrado and deforestation burns in Brazil:BASE-B experiment, *J. Geophys. Res.*, *97*, 14,601–14,619, 1992.

P. E. Artaxo and F. Gerab, Instituto de Físca, USP, C. P. 66318-05389 São Paulo, SP-Brazil.

G. Monroe, Fundação Cearense de Meteorologia e Recursos Hídricos-FUNCEME-C.P.D-322, Fortaleza, CE 60325-Brazil.

E. B. Pereira, M. C. Pereira, and A. W. Setzer, Instituto Nacional de Pesquisas Espaciais/INPE-C.P. 515, S. J. Campos, SP12201-970 Brazil.

(Received August 16, 1995; revised December 20, 1995; accepted December 20, 1995.)